Model-Free Scheme for Angle-of-Attack and Angle-of-Sideslip Estimation

Engineering Notes

Model-Free Scheme for Angle-of-Attack and Angle-of-Sideslip Estimation

Angelo Lerro,* Alberto Brandl,† and Piero Gili‡
Polytechnic University of Turin, 10129 Turin, Italy

https://doi.org/10.2514/1.G005591

I. Introduction

THE recent perspective to improve aviation safety, by means of using synthetic air data on board commercial aviation, opened a new scenario in avionics [1]. In fact, air data sensing is still based on different probes and vanes (used as direct sources of measure) protruding externally from the aircraft fuselage. On the other hand, integrated digital avionics offer the opportunity for air data estimation with data fusion techniques and without using physical (or mechanical) sensors. This approach is also correlated to analytical redundancy [2,3] and can be used as part of a redundant flight control system (FCS) architecture, to monitor physical sensors or to replace failed sensors [4,5], for example.

An air data synthetic sensor, therefore, enables the replacement of a physical sensor with consequent benefits in terms of weight, power consumption, reliability, maintainability and emissions. Air data synthetic sensors can be split into three main categories: 1) pitot-free aircraft speed estimators [6]; 2) vane/sensor-free aerodynamic angle estimators [7,8]; 3) pitot and vane/sensor-free for both airspeed and aerodynamic angle estimators [9]. Using synthetic air data estimation in addition, or in place, of physical air data sensors would also be beneficial for next-generation air vehicles, e.g., unmanned aerial vehicles (UAVs) and urban air mobility (UAM) aircraft, to overcome some issues toward certification [10]. In fact, a redundant air data system (ADS) with limited use of synthetic sensors [11] can lead to a compact solution able to overcome some issues related to common failure modes or incorrect failure diagnosis of modern ADS [12–14].

Although recently re-emerged, the idea of synthetic aerodynamic angle estimators can be dated back to 1949 thanks to the U.S. Air Force (USAF) technical report [15]. In [15] several methods are analyzed to estimate the aerodynamic angles, angle-of-attack (AoA) and angle-of-sideslip (AoS), and one of them was implemented and discussed in 1973 in [16], usually referred to as the Freeman's method. These are considered the first solutions to the problem of the estimation of the aerodynamic angles without using physical sensors. Since then, several other synthetic solutions were conceived [17–24]. The state-of-the-art presented here highlights that synthetic sensors for AoA and AoS estimation can be grouped in two main categories: model based (e.g., Kalman filter) and data driven (e.g., neural networks).

This Note presents a scheme to estimate AoA and AoS. With respect to the state-of-the-art, the proposed scheme is model-free as it does not need any aircraft model or flight test database. Moreover, the latter aspect makes the proposed scheme independent from the aircraft configuration and the flight regime that, instead, it highly affects the design of model-based or data-driven synthetic sensors.

In this work the classical flight mechanic equations are rearranged in order to obtain a scheme that can be solved for AoA and AoS estimation. The proposed scheme is basically a system of nonlinear equations governing the aerodynamic angles based on aircraft dynamics, airspeed, and wind data. To solve the proposed scheme for a preliminary numerical validation, an iterative method has been applied, but several other possibilities exist (e.g., Kalman filters).

In Sec. II notations used in this work are presented. A rearrangement of some flight mechanic equations is introduced in Sec. III, and the problem formulation is presented in Sec. IV. The proposed scheme for aerodynamic angle estimation is derived in Sec. V, and a preliminary numerical verification is presented in Sec. VI before concluding the work.

II. Notations and Reference Frames

In this work, vectors are indicated with bold-italic lower case letters (e.g., $\boldsymbol{v}$), and lower case letters (e.g., v) are used for vector components, whereas the matrices are in bold-italic capital letters (e.g., $\boldsymbol{A}$). An inertial reference frame $\mathcal{F}_I = \{X_I, Y_I, Z_I\}$ is considered, and two noninertial frames are considered centered in the aircraft center of gravity (CG): the body and wind reference frames [25]. The body reference frame $\mathcal{F}_B = \{X_B, Y_B, Z_B\}$ has axes oriented along fixed directions onboard, as in Fig. 1b. The wind reference frame $\mathcal{F}_W = \{X_W, Y_W, Z_W\}$ has the X axis aligned to the freestream velocity vector; the Z axis is the intersection of the plane normal to the trajectory and the (X_B, Z_B) plane of the aircraft and directed downward (i.e., from the upper to the lower wind surface). The aircraft is considered surrounded by an air mass enclosed in a virtual control volume that moves together with its own reference system $\mathcal{F}_{CV} = \{X_{CV}, Y_{CV}, Z_{CV}\}$.

From Fig. 1a the relative distance $\boldsymbol{r}$ between the aircraft and the inertial reference frame can be expressed as $\boldsymbol{r} = \boldsymbol{r}_B + \boldsymbol{r}_W$, where $\boldsymbol{r}_W$ and $\boldsymbol{r}_B$ are, respectively, the distance of the control volume reference system $\mathcal{F}_{CV}$ and the flying object both measured from the origin of the inertial one $\mathcal{F}_I$. In addition, the angular velocity of the frame $\mathcal{F}_B$ with respect to the inertial frame $\mathcal{F}_I$ is

$$\omega = p\hat{\boldsymbol{i}}_B + q\hat{\boldsymbol{j}}_B + r\hat{\boldsymbol{k}}_B$$

where $\hat{\boldsymbol{i}}_B$, $\hat{\boldsymbol{j}}_B$, and $\hat{\boldsymbol{k}}_B$ are the unit vectors in $\mathcal{F}_B$. Recalling the time-derivative properties [26], in the inertial reference frame $\mathcal{F}_I$, the relationship between velocities can be written as

$$\dot{\boldsymbol{r}} = \boldsymbol{v}_I = \dot{\boldsymbol{r}}_B + \boldsymbol{w} \tag{1}$$

where $\boldsymbol{v}_I$ is the inertial velocity, $\dot{\boldsymbol{r}}_B$ is the relative velocity between the aircraft and the surrounding air, and $\boldsymbol{w} = \dot{\boldsymbol{r}}_W$ is the velocity of the control volume, or wind speed. Therefore, the generic flying vehicle is considered to fly with the velocity $\dot{\boldsymbol{r}}_B$, or true air speed, relative to a moving control volume animated by the wind speed $\boldsymbol{w}$, i.e., control volume velocity of the surrounding air in the inertial frame $\mathcal{F}_I$. Finally, the inertial velocity of the aircraft is the vectorial sum of the $\dot{\boldsymbol{r}}_B$ and $\boldsymbol{w}$ as represented in Fig. 1a.

The vector transformation from the inertial reference frame $\mathcal{F}_I$ to the body frame $\mathcal{F}_B$ is obtained considering the ordered sequence 3–2–1 of Euler angles: heading angle ψ, elevation angle θ, and bank angle ϕ. Henceforth, in order to ease the notation, the cosine and sine functions will be denoted as C and S, respectively, whose

Received 7 August 2020; revision received 22 October 2020; accepted for publication 25 October 2020; published online Open Access 30 November 2020.

*Assistant Professor, Department of Mechanical and Aerospace Engineering, C.so Duca degli Abruzzi 24; angelo.lerro@polito.it.

†Research Assistant, Department of Mechanical and Aerospace Engineering, C.so Duca degli Abruzzi 24; alberto.brandl@polito.it.

‡Associate Professor, Department of Mechanical and Aerospace Engineering, C.so Duca degli Abruzzi 24; piero.gili@polito.it.

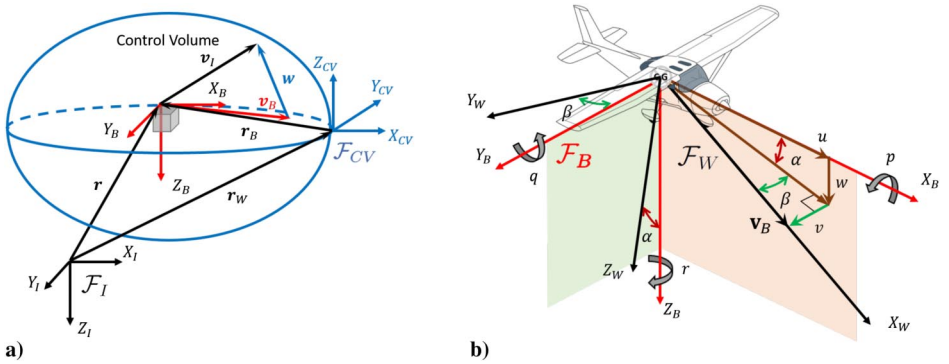

Fig. 1 Representation of a) inertial and control volume reference frames, and b) body and wind reference frames.

arguments are indicated as subscript. The full rotation matrix from $\mathcal{F}_I$ to $\mathcal{F}_B$ is composed as follows:

$$\boldsymbol{C}_{I2B} = \begin{bmatrix} C_\theta C_\psi & C_\theta S_\psi & -S_\theta \\ S_\phi S_\theta C_\psi - C_\phi S_\psi & S_\phi S_\theta S_\psi + C_\phi C_\psi & S_\phi C_\theta \\ C_\phi S_\theta C_\psi + S_\phi S_\psi & C_\phi S_\theta S_\psi - S_\phi C_\psi & C_\phi C_\theta \end{bmatrix} \tag{2}$$

The full rotation matrix from $\mathcal{F}_W$ to $\mathcal{F}_B$ is composed as follows:

$$\boldsymbol{C}_{W2B} = \begin{bmatrix} C_\alpha C_\beta & -C_\alpha S_\beta & -S_\alpha \\ S_\beta & C_\beta & 0 \\ S_\alpha C_\beta & -S_\alpha S_\beta & C_\alpha \end{bmatrix} \tag{3}$$

Among all transformation properties [27], it is worth underlying that

$$\boldsymbol{C}_{I2B}\dot{\boldsymbol{C}}_{B2I} = \boldsymbol{\Omega}_B \tag{4}$$

where

$$\boldsymbol{\Omega}_B = \begin{bmatrix} 0 & -r & q \\ r & 0 & -p \\ -q & p & 0 \end{bmatrix} \tag{5}$$

III. Rearrangement of Flight Mechanic Equations

Recalling velocity definitions [28], Eq. (1) can be rewritten as

$$\boldsymbol{v}_I = \boldsymbol{C}_{B2I}\boldsymbol{v}_B + \boldsymbol{w} \tag{6}$$

and the relative velocity $\boldsymbol{v}_B$ can be obtained from the wind reference frame using Eq. (3) as

$$\boldsymbol{v}_B = V_\infty \hat{\boldsymbol{i}}_{WB} \tag{7}$$

where V_∞ is the magnitude of the relative velocity vector, $V_\infty = |\boldsymbol{v}_B| = \sqrt{u^2+v^2+w^2}$, and $\hat{\boldsymbol{i}}_{WB} = (C_\beta C_\alpha)\hat{\boldsymbol{i}}_B + (S_\beta)\hat{\boldsymbol{j}}_B + (C_\beta S_\alpha)\hat{\boldsymbol{k}}_B$, i.e., the unit vector of the relative velocity in the body reference frame.

Recalling Eqs. (6) and (4), the inertial acceleration $\boldsymbol{a}_I = \dot{\boldsymbol{v}}_I$ projected on the body reference frame can be written as

$$\boldsymbol{a}_B = \boldsymbol{C}_{I2B}\boldsymbol{a}_I = \dot{\boldsymbol{v}}_B + \boldsymbol{\Omega}_B\boldsymbol{v}_B + \boldsymbol{C}_{I2B}\dot{\boldsymbol{w}} \tag{8}$$

Equation (8) highlights the ambiguity coming from inertial acceleration measured onboard. In fact, it can be generated from aircraft maneuver ($\dot{\boldsymbol{v}}_B + \boldsymbol{\Omega}_B\boldsymbol{v}_B$) and/or change in the external wind ($\boldsymbol{C}_{I2B}\dot{\boldsymbol{w}}$). Typically, $\boldsymbol{a}_B$ can be derived onboard from the proper acceleration $\boldsymbol{n}_B$, measured by accelerometers from the Inertial Measurement Unit (IMU), Attitude and Heading Reference System (AHRS), or Inertial Navigation Systems (INS). In this case, the inertial acceleration $\boldsymbol{a}_B$ is calculated as $\boldsymbol{a}_B = \boldsymbol{n}_B - \boldsymbol{C}_{I2B}[0,0,g_0]^T$, where $g_0 \simeq 9.81$ is the gravitational acceleration.

From Eq. (8), the acceleration $\dot{\boldsymbol{v}}_B$ can be written as

$$\dot{\boldsymbol{v}}_B = \boldsymbol{a}_B - \boldsymbol{\Omega}_B\boldsymbol{v}_B - \boldsymbol{C}_{I2B}\dot{\boldsymbol{w}} \tag{9}$$

From Eq. (7), the time derivative of the relative velocity's magnitude is $\dot{V}_\infty = (\boldsymbol{v}_B^T\dot{\boldsymbol{v}}_B/V_\infty)$, and substituting $\dot{\boldsymbol{v}}_B$ with its expression of Eq. (9), the following equation is obtained:

$$\dot{V}_\infty V_\infty = \boldsymbol{v}_B^T\dot{\boldsymbol{v}}_B = \boldsymbol{v}_B^T(\boldsymbol{a}_B - \boldsymbol{\Omega}_B\boldsymbol{v}_B - \boldsymbol{C}_{I2B}\dot{\boldsymbol{w}}) = \boldsymbol{v}_B^T(\boldsymbol{a}_B - \boldsymbol{C}_{I2B})\dot{\boldsymbol{w}} \tag{10}$$

where $\boldsymbol{v}_B^T\boldsymbol{\Omega}_B\boldsymbol{v}_B$ is null, and all terms refer to the same time instant.

IV. Problem Formulation

The proposed scheme is based on the hypothesis that the relative velocity $\boldsymbol{v}_B$ in Eq. (10), and hence the aerodynamic angles, at a certain time instant t can be modeled using information from the past. Therefore, by means of the integral definition, the relative velocity vector $\boldsymbol{v}_B$ at time t can be expressed starting from $\boldsymbol{v}_B$ at a generic time τ, with $t \geq \tau$, as

$$\boldsymbol{v}_B(t) = \boldsymbol{v}_B(\tau) + \int_\tau^t \dot{\boldsymbol{v}}_B(\mathcal{T})\,\mathrm{d}\mathcal{T} \tag{11}$$

Henceforth, the subscript notations $\boldsymbol{v}_{B,t}$ or $(\boldsymbol{v}_B)_t$ are used in place of $\boldsymbol{v}_B(t)$, and the independent variable of the integrand function is omitted in order to ease the notation. Recalling Eq. (9), Eq. (11) can be rewritten as

$$\boldsymbol{v}_{B,t} = \boldsymbol{v}_{B,\tau} + \int_\tau^t (\boldsymbol{a}_B - \boldsymbol{\Omega}_B\boldsymbol{v}_B - \boldsymbol{C}_{I2B}\dot{\boldsymbol{w}})\,\mathrm{d}\mathcal{T} \tag{12}$$

and

$$\boldsymbol{v}_{B,\tau} = \boldsymbol{v}_{B,t} - \int_\tau^t \boldsymbol{a}_B\,\mathrm{d}\mathcal{T} + \int_\tau^t \boldsymbol{\Omega}_B\boldsymbol{v}_B\,\mathrm{d}\mathcal{T} + \int_\tau^t \boldsymbol{C}_{I2B}\dot{\boldsymbol{w}}\,\mathrm{d}\mathcal{T} \tag{13}$$

Replacing $\boldsymbol{v}_{B,\tau}$ with Eq. (13), Eq. (10) can be written at time τ as

$$V_{\infty,\tau}\dot{V}_{\infty,\tau} = \left[\boldsymbol{v}_{B,t} - \int_\tau^t \boldsymbol{a}_B\,\mathrm{d}\mathcal{T} + \int_\tau^t \boldsymbol{\Omega}_B\boldsymbol{v}_B\,\mathrm{d}\mathcal{T} + \int_\tau^t \boldsymbol{C}_{I2B}\dot{\boldsymbol{w}}\,\mathrm{d}\mathcal{T}\right]^T(\boldsymbol{a}_B - \boldsymbol{C}_{I2B}\dot{\boldsymbol{w}})_\tau \Rightarrow$$
$$\Rightarrow V_{\infty,\tau}\dot{V}_{\infty,\tau} + \left[\int_\tau^t \boldsymbol{a}_B\,\mathrm{d}\mathcal{T} - \int_\tau^t \boldsymbol{C}_{I2B}\dot{\boldsymbol{w}}\,\mathrm{d}\mathcal{T}\right]^T(\boldsymbol{a}_B - \boldsymbol{C}_{I2B}\dot{\boldsymbol{w}})_\tau = \left[\boldsymbol{v}_{B,t} + \int_\tau^t \boldsymbol{\Omega}_B\boldsymbol{v}_B\,\mathrm{d}\mathcal{T}\right]^T(\boldsymbol{a}_B - \boldsymbol{C}_{I2B}\dot{\boldsymbol{w}})_\tau \tag{14}$$

where all terms depending on $\boldsymbol{v}_B$, and hence the aerodynamic angles, are collected on the right-hand side.

V. Proposed Scheme

The proposed scheme, named "Angle of Attack and Sideslip Estimator" (ASSE), is based on making dependencies from the relative body velocity $\boldsymbol{v}_B$ explicit. In this case, the integral term $\int_\tau^t \boldsymbol{\Omega}_B \boldsymbol{v}_B \, \mathrm{d}\mathcal{T}$ of Eq. (14) must be explicated in terms of $\boldsymbol{v}_B$. Several levels of approximations can be assumed. In this work, the proposed formulation is based on the assumption that the integrand function is constant in the generic time interval $[\tau, t]$. The latter hypothesis is identified as the zero-order approximation.

A. Zero-Order ASSE Approximation

In a generic time window, from τ to t, the integrand function of $\int_\tau^t \boldsymbol{\Omega}_B \boldsymbol{v}_B \, \mathrm{d}\mathcal{T}$ in Eq. (14) can be approximated constant; therefore

$$\int_\tau^t \boldsymbol{\Omega}_B \boldsymbol{v}_B \, \mathrm{d}\mathcal{T} = (\boldsymbol{\Omega}_B \boldsymbol{v}_B)_t \Delta t \tag{15}$$

where $\Delta t = t - \tau$. Substituting the latter expression into Eq. (14) and recalling matrix properties, Eq. (14) can be rewritten as

$$\begin{aligned} V_{\infty,\tau}\dot{V}_{\infty,\tau} + \left[\int_\tau^t \boldsymbol{a}_B \, \mathrm{d}\mathcal{T} - \int_\tau^t \boldsymbol{C}_{I2B}\dot{\boldsymbol{w}} \, \mathrm{d}\mathcal{T}\right]^T (\boldsymbol{a}_B - \boldsymbol{C}_{I2B}\dot{\boldsymbol{w}})_\tau \\ = V_{\infty,t}\hat{\boldsymbol{i}}_{WB,t}^T (\boldsymbol{I} - \boldsymbol{\Omega}_{B,t}\Delta t)(\boldsymbol{a}_B - \boldsymbol{C}_{I2B}\dot{\boldsymbol{w}})_\tau \end{aligned} \tag{16}$$

Equation (16) is the basic expression of the zero-order scheme referred to the generic time τ where the aerodynamic angles $\alpha(t)$ and $\beta(t)$ are the only unknowns and all other terms are supposed to be measured. Therefore, the aerodynamic angle estimation proposed here is based on direct measure of 1) true airspeed V_∞ and its time derivative $\dot{V}_\infty$, 2) the inertial body acceleration $\boldsymbol{a}_B$ (described in Sec. III), 3) angular rates, and 4) the wind field. As far as the wind field is concerned, the wind velocity is assumed to be known in order to be able to measure the wind acceleration term $\dot{\boldsymbol{w}}$ in Eq. (16). Even though this assumption is not practicable, it is used here to demonstrate the feasibility of the proposed ASSE scheme. For the sake of clarity, conclusion of this work can always be applicable in the case of null, steady wind field or discrete wind change.

B. Zero-Order ASSE Scheme

To simplify the proposed scheme notations, the measurable quantities of Eq. (16) are grouped and denoted as follows:

$$n_\tau = V_{\infty,\tau}\dot{V}_{\infty,\tau} + \left[\int_\tau^t \boldsymbol{a}_B \, \mathrm{d}\mathcal{T} - \int_\tau^t \boldsymbol{C}_{I2B}\dot{\boldsymbol{w}} \, \mathrm{d}\mathcal{T}\right]^T (\boldsymbol{a}_B - \boldsymbol{C}_{I2B}\dot{\boldsymbol{w}})_\tau \tag{17}$$

and

$$\boldsymbol{m}_\tau = V_{\infty,t}(\boldsymbol{I} - \boldsymbol{\Omega}_{B,t}\Delta t)(\boldsymbol{a}_B - \boldsymbol{C}_{I2B}\dot{\boldsymbol{w}})_\tau = h_\tau \hat{\boldsymbol{i}}_B + l_\tau \hat{\boldsymbol{j}}_B + m_\tau \hat{\boldsymbol{k}}_B \tag{18}$$

Therefore, Eq. (16) can be rewritten in a more compact form:

$$n_\tau = \hat{\boldsymbol{i}}_{WB,t}^T \boldsymbol{m}_\tau = h_\tau C_\beta C_\alpha + l_\tau S_\beta + m_\tau C_\beta S_\alpha \tag{19}$$

Equation (19) represents a generic nonlinear scalar equation in two variables $\alpha(t)$ and $\beta(t)$. For the latter reason, the aerodynamic angles are represented without subscripts related to time. Equation (19) can be expanded back in time starting from t to n-th generic τ_i with $i \in [0, 1, \ldots, n]$, where $\tau_0 \equiv t$. Therefore, the following system of $n + 1$ nonlinear equations is obtained:

$$\begin{cases} n_t = \hat{\boldsymbol{i}}_{WB,t}^T \boldsymbol{m}_t = h_t C_\beta C_\alpha + l_t S_\beta + m_t C_\beta S_\alpha \\ n_{\tau_1} = \hat{\boldsymbol{i}}_{WB,t}^T \boldsymbol{m}_{\tau_1} = h_{\tau_1} C_\beta C_\alpha + l_{\tau_1} S_\beta + m_{\tau_1} C_\beta S_\alpha \\ \vdots \\ n_{\tau_n} = \hat{\boldsymbol{i}}_{WB,t}^T \boldsymbol{m}_{\tau_n} = h_{\tau_n} C_\beta C_\alpha + l_{\tau_n} S_\beta + m_{\tau_n} C_\beta S_\alpha \end{cases} \tag{20}$$

Equation (20) is the generic form of the proposed zero-order ASSE scheme based on $n + 1$ equations. In this work, an expansion in the past is considered ($\tau_{i+1} < \tau_i$) but also a forward expansion is equally feasible leading to the same conclusions of the present work. Moreover, it is worth highlighting that no hypothesis are assumed on time spacing of time steps considered here. In fact, even though very uncommon, nonuniform time spacing can be considered and two subsequent equations can also be written for two nonadjacent time steps. This latter aspect can be useful to improve the condition number of the system in Eq. (20).

The nonlinear system of Eq. (20) can be rewritten in a more compact matrix form as

$$\boldsymbol{n}_n = \left(\hat{\boldsymbol{i}}_{WB,t}^T \boldsymbol{\mathcal{M}}_n^T\right)^T = \boldsymbol{\mathcal{M}}_n \hat{\boldsymbol{i}}_{WB,t} \tag{21}$$

where $\boldsymbol{n}_n = [n_t, n_{\tau_1}, \ldots, n_{\tau_n}]^T$ and $\boldsymbol{\mathcal{M}}_n = [\boldsymbol{m}_t^T, \boldsymbol{m}_{\tau_1}^T, \ldots, \boldsymbol{m}_{\tau_n}^T]^T$. As the components of the unit vector are not independent, an extra condition is given by the unit magnitude constraint $\hat{\boldsymbol{i}}_{WB,t}^T \hat{\boldsymbol{i}}_{WB,t} = 1$. Therefore, the nonlinear system of equations based on the zero-order ASSE scheme can be expressed as

$$\begin{cases} 1 = \hat{\boldsymbol{i}}_{WB,t}^T \hat{\boldsymbol{i}}_{WB,t} \\ \boldsymbol{n}_n = \boldsymbol{\mathcal{M}}_n \hat{\boldsymbol{i}}_{WB,t} \end{cases} \tag{22}$$

The most suitable solver can be adopted to solve the system of nonlinear Eq. (22) for AoA and AoS estimation.

C. Solution Existence Conditions

Under the hypothesis that the system of Eq. (22) could be linear, it would be written as

$$\boldsymbol{n}_n^* = \boldsymbol{\mathcal{M}}_n^* \hat{\boldsymbol{i}}_{WB,t} \tag{23}$$

where $\boldsymbol{n}_n^* = [1, \boldsymbol{n}_n^T]^T$ and $\boldsymbol{\mathcal{M}}_n^* = [\hat{\boldsymbol{i}}_{WB,t}^T, \boldsymbol{\mathcal{M}}_n]^T$. If $\boldsymbol{\mathcal{M}}_n^*$ was invertible, and hence $n = 1$ in order to have a square matrix, the ASSE solution would be obtained as

$$\hat{\boldsymbol{i}}_{WB,t} = \boldsymbol{\mathcal{M}}_1^{*-1} \boldsymbol{n}_1^* \tag{24}$$

In other words, if Eq. (23) was solvable, the solution would be obtained as a function of two time steps ($\tau_0 \equiv t$ and τ_1). This condition for a nonlinear problem only sets the minimum number of equations to be considered. Moreover, a nonzero determinant of $\boldsymbol{\mathcal{M}}_n^*$ is required to have a unique solution. The latter consideration is translated in the following two conditions. Firstly, recalling Eqs. (17) and (18), it is clear that the i-th time step τ_i related to uniform flight conditions introduces an equation leading to a null determinant of the $\boldsymbol{\mathcal{M}}_1^*$. Hence, as also observed in [29], the analytical aerodynamic angle estimation (based on a model-free approach) cannot be performed in uniform flight (or trim) conditions. Secondly, the matrix $\boldsymbol{\mathcal{M}}_1^*$ should have a full rank, or, in other words, each considered time step τ_i shall add an independent equation in order to guarantee that $\boldsymbol{\mathcal{M}}_1^*$ has only linearly independent rows. For the latter condition, it is important to have the chance to base the proposed scheme on nonuniform time grids.

Therefore, assuming that Eq. (22) may be linearized, general conditions on the existence of AoA and AoS solutions based on the proposed ASSE scheme are 1) at least two time steps (τ_0 and τ_1) available, 2) not uniform flight conditions, and 3) two independent equations.

VI. Numerical Verification

In this section, the zero-order ASSE scheme is verified using flight simulated data in the presence of a steady wind field. The simulation is not intended to provide an exhaustive performance evaluation but only a numerical demonstration of the proposed scheme based on the zero-order approximation.

A. Maneuver Definition

The numerical validation is performed using a flight simulator, inspired to a two-seat light motorized aircraft. The simulator is based on a coupled six-degree-of-freedom nonlinear aircraft model equipped with nonlinear aerodynamic and thrust models designed accordingly to flight test results and the engine datasheet. The simulation is run using the explicit Euler scheme with fixed time step $\Delta t = 0.1$ milli/second.

Two different maneuvers are designed in order to excite both longitudinal and lateral-directional modes beyond their linearity: 1) a stall maneuver, described in Fig. 2; 2) a sideslip angle sweep maneuver, described in Fig. 3. Both maneuvers begin in trim conditions. Aileron commands are maintained to their trim positions even though, due to gyroscopic effects, the trim flight condition is not perfectly symmetric. For this latter reason, the aileron during the trim condition is nonzero and both longitudinal and lateral-directional modes are always slightly coupled.

After a short dive, the stall maneuver is performed acting on the sole elevator command, as described in Fig. 2a, producing initially an increase of airspeed and then a smooth deceleration leading to high angle of attack, as can be seen in Fig. 2b, with limited changes in angle of sideslip.

The sideslip angle sweep maneuver is performed acting on the sole rudder command, as described in Fig. 3a, exciting the angle of sideslip in a large range, whereas the speed and the angle of attack are almost constant as can be seen in Fig. 3b.

B. Numerical Results

As described in Sec. V.A, AoA and AoS are estimated simultaneously using the proposed scheme of Eq. (22). Therefore, AoA and AoS estimation is based on measures of 1) true airspeed, 2) true airspeed time derivative, 3) inertial body acceleration, 4) Euler angles (implicitly used to obtain $\boldsymbol{a}_B$ from $\boldsymbol{n}_B$ as described in Sec. IV), 5) body angular rates, and 6) wind acceleration. The simulation does not implement any sensor noise or time delay, and hence all signals used to solve the proposed scheme are noise-free and synchronized.

Even though the system of two equations is the minimum condition to solve the proposed scheme of Eq. (22) as discussed in Sec. V.A, several numbers of nonlinear equations are considered here: 1) two equations written for current time t and a single past time $\tau_1 = t - \Delta t$; 2) three equations written for current time t and a two past times $\tau_1 = t - \Delta t$ and $\tau_2 = t - 2\Delta t$; and 3) four equations written for current time t and a three past times $\tau_1 = t - \Delta t$, $\tau_2 = t - 2\Delta t$, and $\tau_3 = t - 3\Delta t$.

In this work, each system of nonlinear equations is solved using an iterative method based on the Levenberg–Marquardt algorithm [30]. Because of importance of the first guess in iteration methods, the proposed scheme is applied with the following strategy: 1) using the AoA/AoS values previously estimated as initial condition, and 2) only the very first iteration (i.e., from the trim condition) is initialized by imposing AoA and AoS true values.

Using the proposed scheme, synthetic estimations of aerodynamic angles are reported in Fig. 4 for the stall maneuver and in Fig. 5 for the sideslip sweep maneuver. A general good agreement can be observed between the true values and the aerodynamic angle estimations. In fact, it can be noted that, although the maximum absolute error is smaller than 0.6° for both maneuvers, there are few error peaks mainly related to the zero-order approximation used with the proposed scheme as it will be shown later in Sec. VI.C. These numerical results confirm the validity of the proposed scheme to estimate aerodynamic angles during maneuvered flight conditions with at least two equations.

By extending the proposed scheme to three and four equations, the estimation accuracy is not increased significantly and sometimes higher errors are shown as in Fig. 5a. On the contrary, in Fig. 4b, it can be noted that the estimation accuracy of the four-equation-scheme is only slightly improved if compared with the two-equation-scheme. If increasing the number of equations introduces more conditions to the proposed scheme, on the other side, as shown later in Sec. VI.C,

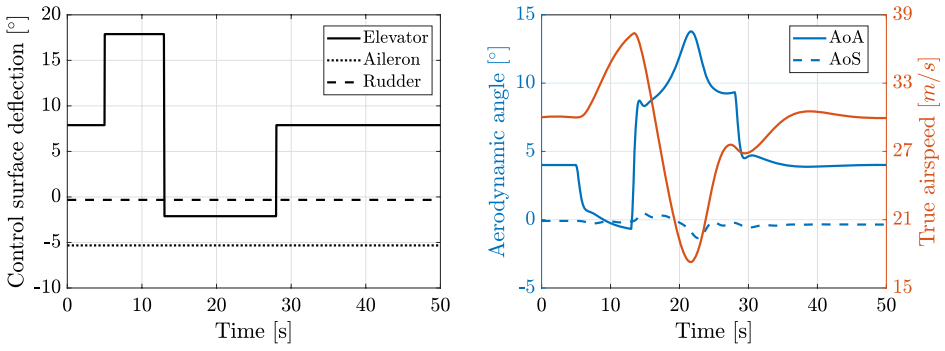

a) b)

Fig. 2 Input–output scenario for a stall maneuver: a) more relevant input commands and b) main output data.

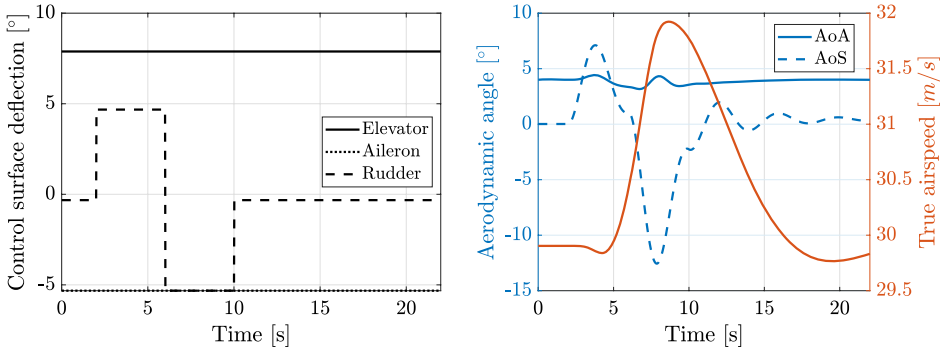

a) b)

Fig. 3 Input–output scenario for sideslip angle sweep maneuver: a) more relevant input commands and b) main output flight data.

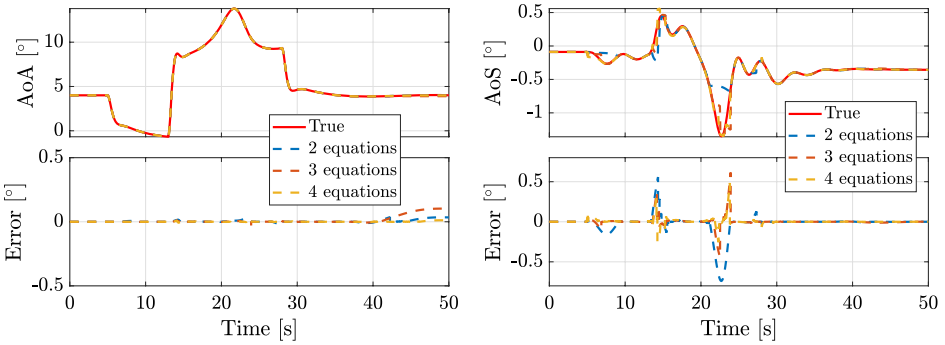

Fig. 4 Estimation using the proposed scheme with two, three, and four equations during the stall maneuver: a) angle of attack and b) angle of sideslip.

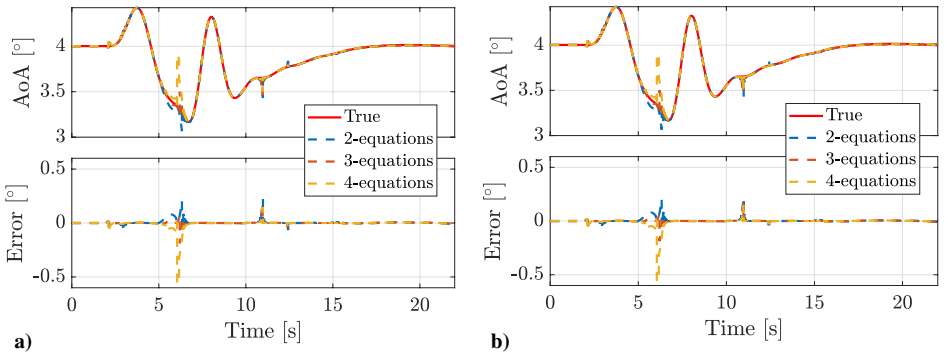

Fig. 5 Estimation using the proposed scheme with two, three, and four equations during the angle of sideslip sweep: a) angle of attack and b) angle of sideslip.

the zero-order approximation always introduces smaller errors for the two-equation scheme. As far as the preliminary numerical validation is concerned, the two-equation-scheme seems preferable because the mathematical complexity introduced with the three- and four-equation schemes is not supported by significant accuracy improvement.

C. Zero-Order ASSE Approximation Error

To evaluate the error introduced with the zero-order ASSE scheme in the system of Eq. (22), the exact value of the integral term of Eq. (15) is compared with zero-order approximation. Recalling Eq. (14) and under the assumption of steady wind field, the zero-order ASSE approximation error (0-OAE) is calculated as

$$\text{0-OAE} = -\frac{((\boldsymbol{\Omega}_B \boldsymbol{v}_B)_t \Delta t - \int_\tau^t \boldsymbol{\Omega}_B \boldsymbol{v}_B \, \mathrm{d}\mathcal{T})\boldsymbol{a}_B}{(\int_\tau^t \boldsymbol{\Omega}_B \boldsymbol{v}_B \, \mathrm{d}\mathcal{T})\boldsymbol{a}_B} \tag{25}$$

Although the large range of the flight maneuver described before, Fig. 6 shows that the zero-order ASSE approximation errors are limited in time (shorter than 0.25 s) and the largest errors are introduced as the number of equations is increased. The latter aspect is straightforward because the integrand function of Eq. (15) is considered constant for a longer time. The maximum absolute 0-OAE is bounded within ±6% for the system of four equations, whereas 0-OAE is reduced to ±2% for the system of two equations. The highest 0-OAE values are shown at the beginning of the maneuver, i.e., at the transition between steady state and dynamic flight conditions.

VII. Conclusions

In the field of aerodynamic angle synthetic estimators, this Note introduces a model-free scheme for concurrent angle-of-attack and angle-of-sideslip estimation independent from the aircraft. After a rearrangement of classical flight mechanic equations, a simplification hypothesis is applied in order to obtain a set of nonlinear equations, or the zero-order ASSE scheme. The scheme is based on the measure of true airspeed, angular rates, inertial accelerations, aircraft attitudes, and wind acceleration vector. Each equation refers to a different time instant. The proposed scheme shall be based at least on two equations written for dynamic conditions. In fact, the proposed scheme

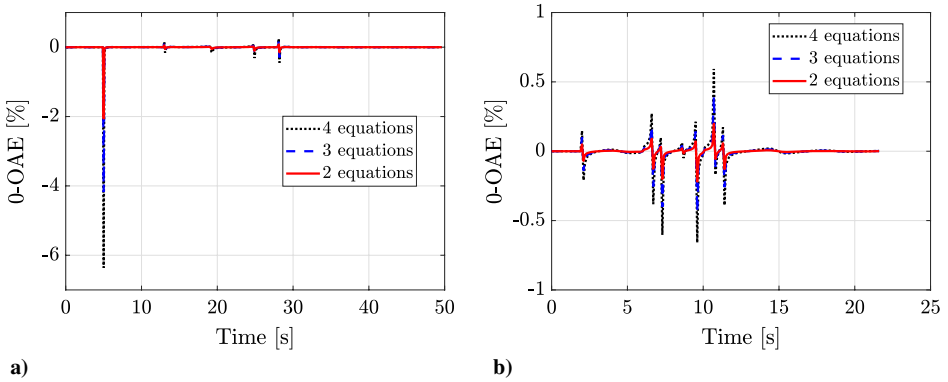

Fig. 6 Zero-order ASSE approximation error (0-OAE) for a) stall and b) sideslip angle sweep maneuvers.

is only applicable when the aircraft is maneuvering, whereas for trim conditions the scheme is not applicable. The proposed zero-order approximation does not introduce significant errors with respect to the corresponding exact value even if the approximation error increases with the number of equations. From a preliminary numerical validation, the proposed scheme demonstrates a good accuracy in aerodynamic angle estimation during simulated flight conditions. The solver of the proposed scheme is not limited to the iterative method used in this Note. Moreover, from the analysis of numerical results, the estimation accuracy is not significantly improved by increasing the number of equations. Therefore, for the zero-order scheme, the best tradeoff is obtained using only two equations.

References

[1] Flottau, J., "Boeing 737 MAX Return Decision in January," *Aviation Week & Space Technology*, 2019, https://aviationweek.com/air-transport/easas-director-expects-boeing-737-max-return-decision-january.

[2] Gertler, J., "Analytical Redundancy Methods in Fault Detection and Isolation—Survey and Synthesis," *IFAC Proceedings Volumes*, Vol. 24, No. 6, 1991, pp. 9–21; also *iFAC/IMACS Symposium on Fault Detection, Supervision and Safety for Technical Processes (SAFEPROCESS'91)*, Baden-Baden, Germany, Sept. 1991. https://doi.org/10.1016/S1474-6670(17)51119-2

[3] Perhinschi, M., Campa, G., Napolitano, M., Lando, M., Massotti, L., and Fravolini, M., "Modelling and Simulation of a Fault-Tolerant Flight Control System," *International Journal of Modelling and Simulation*, Vol. 26, No. 1, 2006, pp. 1–10. https://doi.org/10.1080/02286203.2006.11442345

[4] Pouliezos, A. D., and Stavrakakis, G. S., "Analytical Redundancy Methods," *Real Time Fault Monitoring of Industrial Processes*, Vol. 12, Springer, Dordrecht, The Netherlands, 1994, pp. 93–178. https://doi.org/10.1007/978-94-015-8300-8_2

[5] Rhudy, M. B., Fravolini, M. L., Porcacchia, M., and Napolitano, M. R., "Comparison of Wind Speed Models Within a Pitot-Free Airspeed Estimation Algorithm Using Light Aviation Data," *Aerospace Science and Technology*, Vol. 86, March 2019, pp. 21–29. https://doi.org/10.1016/j.ast.2018.12.028

[6] Rhudy, M. B., Larrabee, T., Chao, H., Gu, Y., and Napolitano, M., "UAV Attitude, Heading, and Wind Estimation Using GPS/INS and an Air Data System," *AIAA Guidance, Navigation, and Control (GNC) Conference*, AIAA Paper 2013-5201, 2013, pp. 1–11. https://doi.org/10.2514/6.2013-5201

[7] Lerro, A., Brandl, A., Battipede, M., and Gili, P., "Preliminary Design of a Model-Free Synthetic Sensor for Aerodynamic Angle Estimation for Commercial Aviation," *Sensors*, Vol. 19, No. 23, 2019, p. 5133. https://doi.org/10.3390/s19235133

[8] Colgren, R., Frye, M., and Olson, W., "A Proposed System Architecture for Estimation of Angle-of-Attack and Sideslip Angle," *Guidance, Navigation, and Control Conference and Exhibit*, AIAA Paper 1999-4078, 1999, pp. 743–750. https://doi.org/10.2514/6.1999-4078

[9] Lie, F. A. P., and Gebre-Egziabher, D., "Sensitivity Analysis of Model-Based Synthetic Air Data Estimators," *AIAA Guidance, Navigation, and Control Conference*, AIAA Paper 2015-0081, 2015, pp. 1–18. https://doi.org/10.2514/6.2015-0081

[10] European Aviation Safety Agency, EASA, "Proposed Means of Compliance with the Special Condition VTOL," May 2020. MOC SC-VTOL issue 1.

[11] Lerro, A., Battipede, M., Gili, P., Ferlauto, M., Brandl, A., Merlone, A., Musacchio, C., Sangaletti, G., and Russo, G., "The Clean Sky 2 MIDAS Project—An Innovative Modular, Digital and Integrated Air Data System for Fly-by-Wire Applications," *2019 IEEE 5th International Workshop on Metrology for AeroSpace (MetroAeroSpace)*, Vol. 1, IEEE, New York, 2019, pp. 714–719. https://doi.org/10.1109/MetroAeroSpace.2019.8869602

[12] Eubank, R., Atkins, E., and Ogura, S., "Fault Detection and Fail-Safe Operation with a Multiple-Redundancy Air-Data System," *AIAA Guidance, Navigation, and Control Conference*, AIAA Paper 2010-7855, 2010. https://doi.org/10.2514/6.2010-7855

[13] Lu, P., Van Eykeren, L., Van Kampen, E.-J., and Chu, Q., "Air Data Sensor Fault Detection and Diagnosis with Application to Real Flight Data," *AIAA Guidance, Navigation, and Control Conference, AIAA SciTech Forum*, AIAA Paper 2015-1311, 2015. https://doi.org/10.2514/6.2015-1311

[14] "Aircraft Accident Investigation Report—PT. Lion Mentari Airlines Boeing 737-8 (MAX)," *Komite Nasional Keselamatan Transportasi Republic of Indonesia*, KNKT.18.10.35.04, 2018.

[15] Dendy, J., and Transier, K., "Angle-of-Attack Computation Study," Air Force Flight Dynamics Lab. AFFDL-TR-69-93, 1969.

[16] Freeman, D. B., "Angle of Attack Computation System," Air Force Flight Dynamics Lab. AFFDL-TR-73-89, 1973.

[17] Rohloff, T. J., Whitmore, S. A., and Catton, I., "Air Data Sensing from Surface Pressure Measurements Using a Neural Network Method," *AIAA Journal*, Vol. 36, No. 11, 1998, pp. 2094–2101. https://doi.org/10.2514/2.312

[18] Samara, P. A., Fouskitakis, G. N., Sakellariou, J. S., and Fassois, S. D., "Aircraft Angle-of-Attack Virtual Sensor Design via a Functional Pooling Narx Methodology," *2003 European Control Conference (ECC)*, Vol. 1, Inst. of Electrical and Electronics Engineers, New York, 2003, pp. 1816–1821. https://doi.org/10.23919/ECC.2003.7085229

[19] Wise, K. A., "Computational Air Data System for Angle-of-Attack and Angle-of-Sideslip," U.S. Patent 6,928,341 B2, 2005.

[20] Langelaan, J. W., Alley, N., and Neidhoefer, J., "Wind Field Estimation for Small Unmanned Aerial Vehicles," *Journal of Guidance, Control, and Dynamics*, Vol. 34, No. 4, 2011, pp. 1016–1030. https://doi.org/10.2514/1.52532

[21] Lerro, A., Battipede, M., Gili, P., and Brandl, A., "Aerodynamic Angle Estimation: Comparison Between Numerical Results and Operative Environment Data," *CEAS Aeronautical Journal*, Vol. 11, No. 1, 2020, pp. 249–262. https://doi.org/10.1007/s13272-019-00417-x

[22] Lu, P., Van Eykeren, L., van Kampen, E., de Visser, C. C., and Chu, Q. P., "Adaptive Three-Step Kalman Filter for Air Data Sensor Fault Detection and Diagnosis," *Journal of Guidance, Control, and Dynamics*, Vol. 39, No. 3, 2016, pp. 590–604. https://doi.org/10.2514/1.G001313

[23] Prem, S., Sankaralingam, L., and Ramprasadh, C., "Pseudomeasurement-Aided Estimation of Angle of Attack in Mini Unmanned Aerial Vehicle," *Journal of Aerospace Information Systems*, Vol. 17, No. 11, 2020, pp. 603–614. https://doi.org/10.2514/1.I010783

[24] Valasek, J., Harris, J., Pruchnicki, S., McCrink, M., Gregory, J., and Sizoo, D. G., "Derived Angle of Attack and Sideslip Angle Characterization for General Aviation," *Journal of Guidance, Control, and Dynamics*, Vol. 43, No. 6, 2020, pp. 1039–1055. https://doi.org/10.2514/1.G004010

[25] Etkin, B., and Reid, L., *Dynamics of Flight: Stability and Control*, 3rd ed., Wiley, New York, 1995.

[26] Britting, K., *Inertial Navigation Systems Analysis*, Wiley Canada, Norwood, 1971.

[27] Salychev, O. S., *Applied Inertial Navigation: Problems and Solutions*, BMSTU Press, Moscow, Russia, 2004.

[28] Nelson, R., *Flight Stability and Automatic Control*, McGraw–Hill Series in Aeronautical and Aerospace Engineering, McGraw–Hill Ryerson, Boston, 1989.

[29] Sun, K., Regan, C. D., and Egziabher, D. G., "GNSS/INS Based Estimation of Air Data and Wind Vector Using Flight Maneuvers," *2018 IEEE/ION Position, Location and Navigation Symposium (PLANS)*, Inst. of Electrical and Electronics Engineers, New York, 2018, pp. 838–849. https://doi.org/10.1109/PLANS.2018.8373461

[30] Marquardt, D. W., "An Algorithm for Least-Squares Estimation of Nonlinear Parameters," *Journal of the Society for Industrial and Applied Mathematics*, Vol. 11, No. 2, 1963, pp. 431–441. https://doi.org/10.1137/0111030